nature protocols

PROTOCOL

https://doi.org/10.1038/s41596-021-00532-2

Check for updates

Surgical implantation of wireless, battery-free optoelectronic epidural implants for optogenetic manipulation of spinal cord circuits in mice

Jose G. Grajales-Reyes[1,2], Bryan A. Copits[1], Ferrona Lie[3,4], Yongjoon Yu[3], Raudel Avila[4], Sherri K. Vogt[1], Yonggang Huang[4,5,6], Anthony R. Banks[3,5,6], John A. Rogers[5,6], Robert W. Gereau IV[1]✉ and Judith P. Golden[1]✉

The use of optogenetics to regulate neuronal activity has revolutionized the study of the neural circuitry underlying a number of complex behaviors in rodents. Advances have been particularly evident in the study of brain circuitry and related behaviors, while advances in the study of spinal circuitry have been less striking because of technical hurdles. We have developed and characterized a wireless and fully implantable optoelectronic device that enables optical manipulation of spinal cord circuitry in mice via a microscale light-emitting diode (μLED) placed in the epidural space (NeuroLux spinal optogenetic device). This protocol describes how to surgically implant the device into the epidural space and then analyze light-induced behavior upon μLED activation. We detail optimized optical parameters for in vivo stimulation and demonstrate typical behavioral effects of optogenetic activation of nociceptive spinal afferents using this device. This fully wireless spinal μLED system provides considerable versatility for behavioral assays compared with optogenetic approaches that require tethering of animals, and superior temporal and spatial resolution when compared with other methods used for circuit manipulation such as chemogenetics. The detailed surgical approach and improved functionality of these spinal optoelectronic devices substantially expand the utility of this approach for the study of spinal circuitry and behaviors related to mechanical and thermal sensation, pruriception and nociception. The surgical implantation procedure takes ~1 h. The time required for the study of behaviors that are modulated by the light-activated circuit is variable and will depend upon the nature of the study.

Introduction

The development of optogenetic approaches for manipulation of neuron activity with spatial and temporal precision in combination with the advancement in techniques for defining and accessing specific populations of neurons on the basis of genetic markers has revolutionized our understanding of a number of complex circuits in the brain[1,2]. However, wireless optogenetic approaches designed to manipulate spinal circuits are not as advanced as those currently used to modulate circuits in the brain. We describe here a wireless optogenetic approach for the modulation of spinal circuitry and for the analysis of behavior mediated by these circuits[3–6]. The protocol details the methods required for use of the NeuroLux spinal optogenetic device (www.neurolux.org) for stimulation of spinal afferents in mice. The procedure has two main stages: surgical implantation of the microscale light-emitting diode (μLED) device (Steps 1–26) and optogenetic activation of spinal afferents to elicit and document behavior (Steps 27–29).

Development of the protocol

In 2015, we described a fully implantable, battery-free wireless optoelectronic device designed to evaluate sensory behaviors induced by optical activation of spinal afferents and to interrogate spinal cord circuitry[4]. In 2017, we improved the design of this device by implementing near-field communication powering[3]. Our previous publications represent important advances in the development of tools designed to study spinal cord circuitry and sensory behavior using optogenetics. However,

[1]Washington University Pain Center and Department of Anesthesiology, Washington University School of Medicine, St. Louis, MO, USA. [2]Medical Scientist Training Program, Washington University in St. Louis, St. Louis, MO, USA. [3]NeuroLux Inc., Evanston, IL, USA. [4]Department of Mechanical Engineering, Evanston, IL, USA. [5]Department of Materials Science and Engineering, Northwestern University, Evanston, IL, USA. [6]Department of Neuroscience and Affiliated Faculty, Northwestern University, Evanston, IL, USA. ✉e-mail: gereaur@wustl.edu; jgolden@wustl.edu

a number of confounds, which limited the use of this technology, remain to be addressed. In this protocol, we have addressed these limitations by improving both the design of the spinal device and the procedures for implantation and use of the device. In previous work, we used an earlier version of the spinal device to activate nociceptive spinal afferents that expressed channelrhodopsin-2 (ChR2), an excitatory light-activated channel, and observed acute (≤1 d after device implantation) light-induced aversive behaviors that included nonspecific behaviors such as vocalization and jumping[3]. Here we demonstrate robust dermatome-appropriate nocifensive behaviors induced by optogenetic activation of the central terminals of nociceptive afferents at the level of the dorsal spinal cord. These behaviors can be elicited for at least 4 weeks after implantation of the spinal optoelectronic device and are blocked by the analgesic buprenorphine, indicating that the observed responses represent nocifensive behaviors. We also demonstrate that long-term device implantation does not alter mechanical- or cold-evoked sensory behavior.

The sections below describe critical changes to the design of the spinal optogenetic device, the surgical implantation procedure and the stimulation parameters, all of which have substantially improved the function of the device.

Design and functionality of the spinal optogenetic device

In our recent work, we introduced wireless implantable devices for spinal optogenetics with mechanically robust and overall thin, flexible form factor with dimensions 10 × 5 × 0.2 mm (length × width × thickness)[3]. The rectangular coil designated for wireless power harvesting consists of seven planar loops with 50 mm pitch (Fig. 1, Supplementary Fig. 1, Table 1). The updated device described in this protocol has similar characteristics and dimensions (11.9 × 5.07 × 0.15 mm, copper traces: seven turns, 60 μm width, 50 μm spacing). Modifications include rounded edges, and printed board circuits optimized for mass manufacturing (Fig. 1a–f, Table 1). The transmission coil and probe are composed of a polyimide, copper, polyimide, copper, polyimide (PI/Cu/PI/Cu/PI, 12.5/18/50/18/12.5 μm thickness, Uniflex) layer that is commercially available. The outside layer of the electronic components is coated with poly(dimethylsiloxane) (PDMS, 0.5–300 μm). An encapsulating layer of parylene (14 μm) covering all surfaces of the device is deposited using a simple commercial process (Plasma Ruggedized Solutions). An additional Schottky diode (Digikey, cat. no. CDBZ0130R-HF) is added to the initial electronic circuits, creating a two Schottky diode setup with low forward voltage thresholds for rectifying the alternating current signal such that passage through a smoothing capacitor (2.2 μF; Murata Electronics, cat. no. GRM033R61A225KE47D) produces a stable direct current voltage. Having two Schottky diodes controls the current flow in the μLED, ensuring isolation of the μLED from voltage variations on the coil. The two-diode half-bridge rectifier setup reduces the high-frequency noise component at the input of the linear dropout regulator and stabilizes the operation. The low internal capacitance of these diodes (0.2 pF) at 13.56 MHz minimizes losses in the rectifier. Additional benefits include isolation of the resonant circuit from the digital electronics (Table 1). Further details regarding device design and function are provided in Supplementary Methods and Supplementary Figs. 1–6.

Device implantation surgery

Surgical procedures for implantation of biomedical devices initiate an inflammatory response triggered by injury to vasculature and other tissue in the region of device implantation. This response can compromise the function of implanted devices[7]. Previously, we performed implantation of the optogenetic spinal device with the μLED positioned immediately above a partial laminectomy of the dorsal T13 vertebra[3]. We found that positioning of the μLED close to the laminectomy site, where considerable bleeding occurs, resulted in the growth of inflammatory tissue on and around the μLED. We suspected that the deposit of inflammatory tissue in the vicinity of the μLED caused scattering of the light from the μLED, resulting in the attenuation of light-evoked pain behavior observed after postimplantation day (PID) 1 in our previous report[3]. Here we have modified the implantation procedure such that the μLED is positioned in the epidural space under the T13 vertebra, which is several millimeters distant from the laminectomy site (Fig. 2a–e). This modification substantially improved the function of the device such that we are now able to consistently elicit light-evoked behaviors for more than 4 weeks postimplantation. We have also minimized inflammation by thoroughly irrigating the surgical field with sterile saline to remove blood and other tissue debris.

Stimulation parameters

The updated stimulation parameters used in this protocol are selected based on ex vivo spinal cord slice recordings. We used patch clamp electrophysiology in spinal cord slice preparations to record

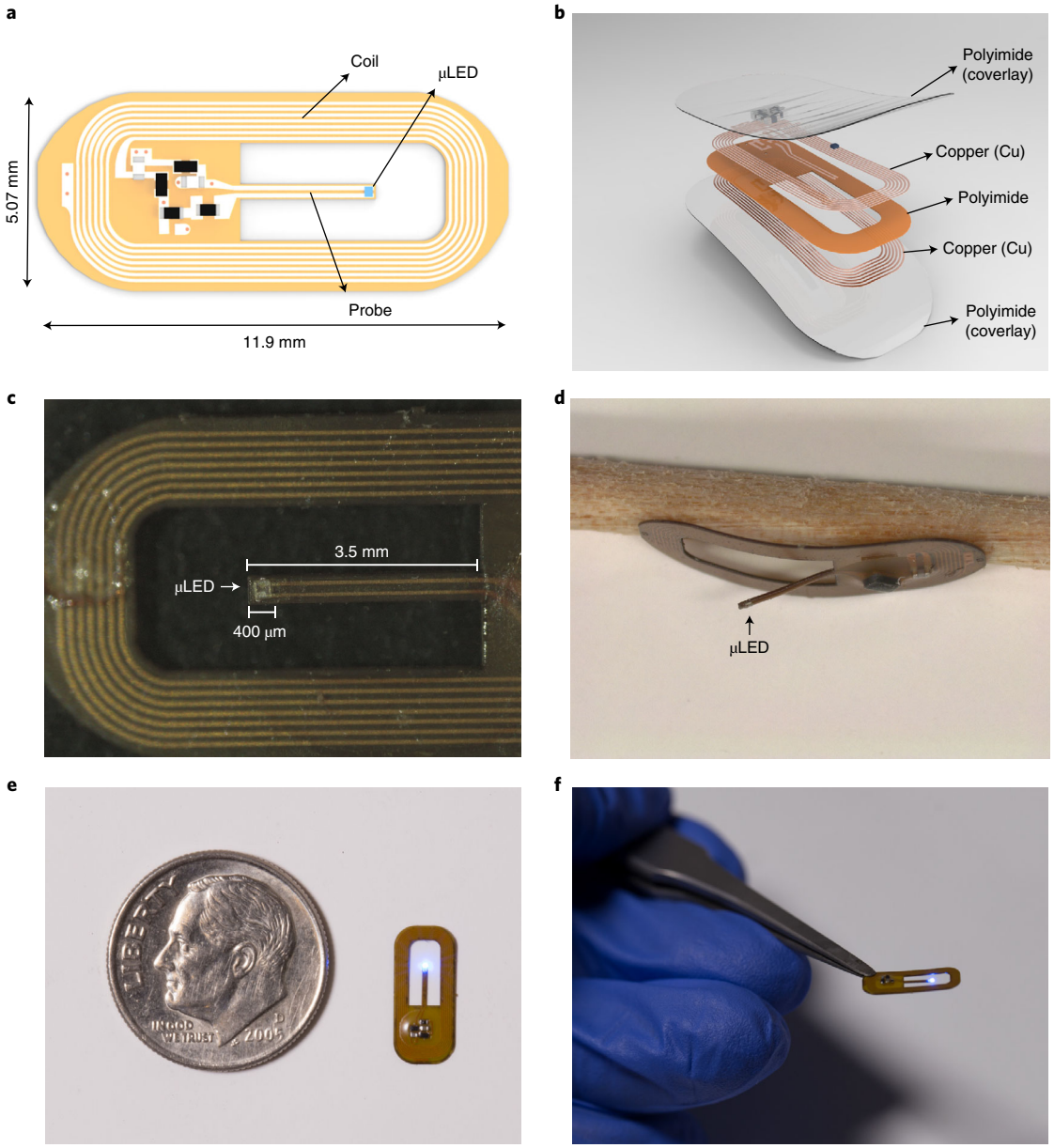

Fig. 1 | Schematics of the updated spinal optogenetic device. a, A two-dimensional view of the spinal μLED device with dimensions (length 11.9 mm × width 5.07 mm). **b**, Exploded view of the spinal μLED device illustrating device layers. **c**, Magnified image of the spinal μLED device showing the size of the μLED (400 μm) and the length of the μLED probe (3.5 mm). **d**, Magnified image of a spinal μLED device illustrating the conformation of the device required for implantation. **e**, Image showing the size of a spinal μLED implant in relation to a dime. **f**, Image showing a spinal μLED device grasped with forceps to demonstrate proper handling with Dumont forceps.

excitatory postsynaptic currents in spinal dorsal horn neurons that were induced by optical stimulation of transient receptor potential cation channel subfamily V member 1 (TRPV1)-lineage nociceptive primary afferents expressing ChR2 (Fig. 3a,b)[8–10]. We found that short bright pulses (1, 2 and 5 ms pulses) were effective for optical activation of ChR2+ central projections (Fig. 3c–e). We selected lower frequencies (1–5 Hz) for stimulation of nociceptive primary afferents based on reported in vivo recordings of dorsal root ganglion neurons from naïve and injured animals[8,9]. This modification has resulted in more effective, and potentially more physiological, activation of nociceptive afferents, as evidenced by the robust and dermatome specific pain behaviors observed at lower stimulation frequencies. The ex vivo spinal cord slice recording experiments have also confirmed that the stimulation pulse width and optical power output used previously are effective for activating nociceptive afferents[3].

Table 1 | Characteristics of the spinal µLED device

Category	Device used in Samineni et al. (2017)[3]	Updated device used here
Image		
Overall dimensions (length × width × thickness)	10 × 5 × 0.20 mm	12 ×5 × 0.15 (0.45, if considering SMD components) mm
Probe dimensions	L: 3.5 mm, W: 400 µm	L: 3.5 mm, W: 400 µm
Flex	Cu/PI/Cu (18/50/18 µm)	PI/Cu/PI/Cu/PI (12.5/18/50/18/12.5 µm)
Encapsulation	Polyisobutylene, PDMS	PDMS (10 µm), parylene-C (14 µm)
Components	Capacitor (40 pF; Murata Electronics, cat. no. 250R05L220GC4T), Schottky diode (Comchip Technology, cat. no. CBDQR0130L-HF)	Capacitor (56 pF; Johanson Technology, cat. no. 250R05L560JV4T), Schottky diode (Comchip Technology, d1, D2; cat. no. CDBZ0130R-HF), resistor (R1, 0 ohm; cat. no. P15979CT-ND), Digikey capacitor (C2, 2.2 µF; Murata, cat. no. 0201 GRM033R661A225KE47D)

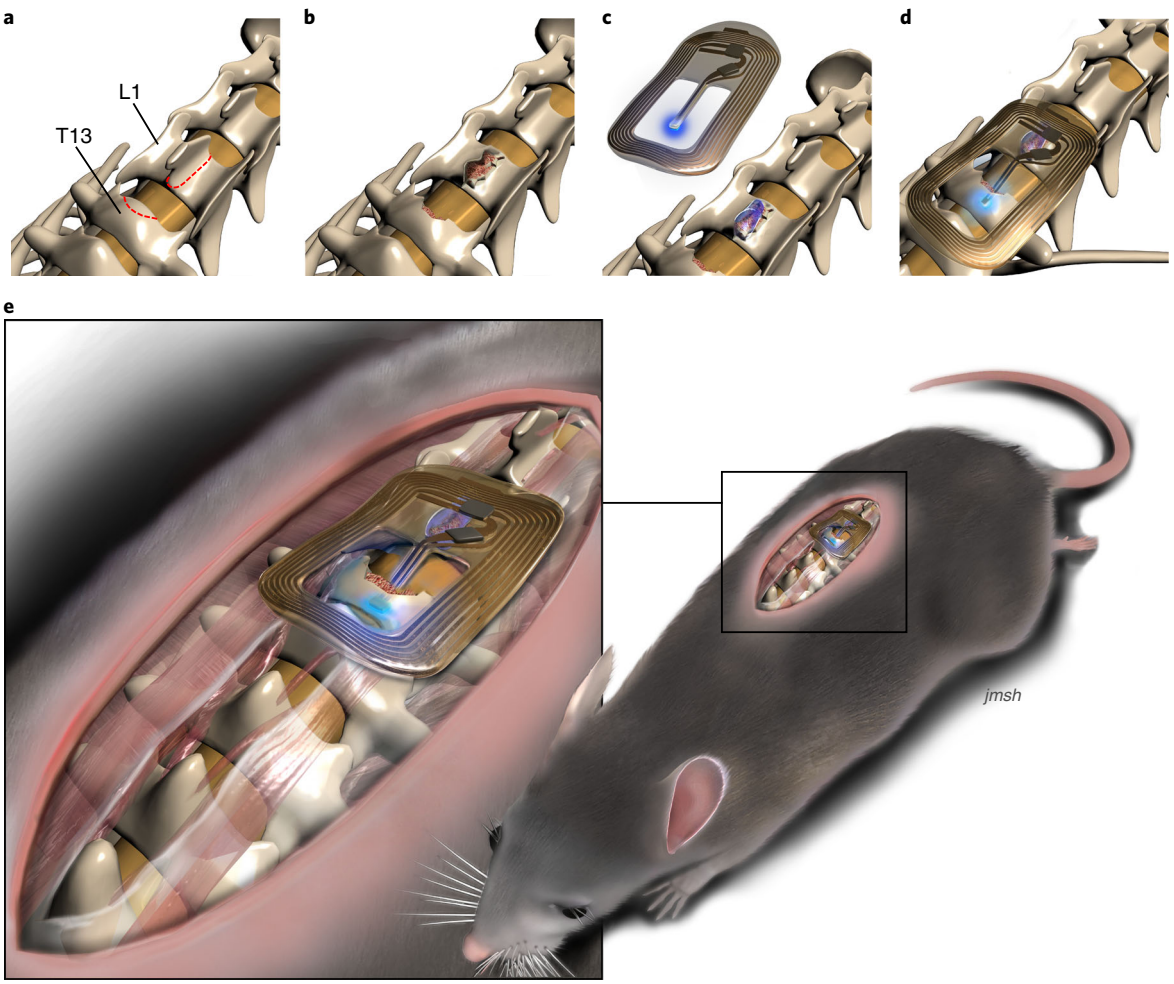

Fig. 2 | Graphical representation of the surgical procedure for implantation of the spinal µLED device. a, Anatomical illustration of the vertebral column with the sites of bone removal outlined (dashed red outlines) on the T13 vertebral bone (laminectomy) and the L1 vertebral bone (spinous process removal). **b**, Partial laminectomy at T13 and spinous process of L1 removed. **c**, Orientation of the µLED implant in relation to the vertebral column, with the probe oriented rostrally and the µLED facing the dura over the spinal cord. **d**, Insertion of the µLED implant under the T13 vertebra. **e**, Large-scale image of a completed µLED implant. Mouse illustration by Janet M. Sinn-Hanlon.

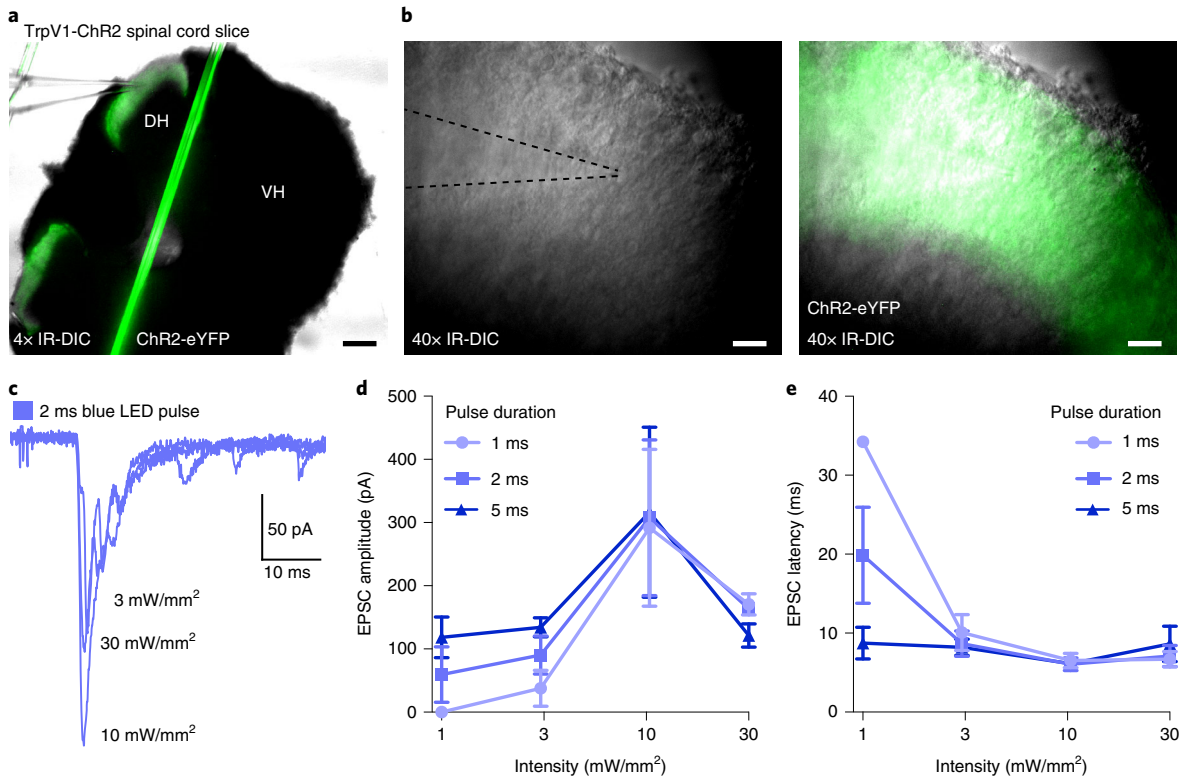

Fig. 3 | Electrophysiological characterization of light-induced activation of TrpV1+ primary afferents in an ex vivo spinal cord slice preparation. **a**, Low magnification image of the spinal cord slice preparation from a TrpV1-ChR2 mouse showing an overlay of the differential interference contrast (DIC) image with a fluorescent image showing ChR2-eYFP expression (scale bar 200 µm). **b**, Higher magnification illustration of a differential interference contrast image (DIC, left panel) and an overlay of the DIC image with a fluorescent image (right panel) showing ChR2-eYFP expression in a spinal cord slice preparation (scale bar 20 µm). **c**, Representative inward photocurrents evoked by blue LED illumination at different light intensities. **d**, Characterization of the amplitude (pA) of optically evoked postsynaptic currents (EPSC) at different light intensities while varying the pulse duration (ms). **e**, Characterization of the latency of optically evoked postsynaptic currents (EPSC) at different power outputs while varying the pulse duration. DH, spinal dorsal horn, VH, spinal ventral horn. Error bars represent standard error of the mean ($n = 2$–8 replicates). The full quantitative data for panels **d** and **e** are provided in the Source Data associated with this protocol. Experiments shown in this figure comply with the guidelines and policies of the Animal Care and Use Committee of Washington University School of Medicine regarding the use of vertebrate animals in research.

The critical advancements described in this protocol have substantially improved the functionality of these spinal µLED optogenetic devices. These improvements in functionality include the ability to achieve light-evoked behavior that is directed to specific areas of the body that are innervated by afferents with central projections at the level of the lumbar enlargement in the spinal column where the µLED is located. In addition, we are now able to elicit light-evoked behaviors for longer than 4 weeks postimplantation, which will facilitate the study of chronic conditions including neuropathic pain. These advancements expand the potential utility of this technology to include studies of sensory behavior, analysis of spinal circuits and efficient evaluation of the analgesic efficacy of novel drugs.

Applications of the protocol

Spinal circuitry characterization

The use of optogenetics has revolutionized the study of complex neural circuits and related behaviors[4,11,12]. Transgenic mouse lines that permit the selective expression of opsins in specific populations of spinal neurons or in spinal afferents from the periphery or the brain, in conjunction with our µLED spinal optogenetic device, can be utilized to characterize spinal cord circuits using anatomical and behavioral readouts[13,14].

Sensory and pain behavior studies

In combination with transgenic mice that express optogenetic channels in specific afferent or spinal neuron populations, the spinal optoelectronic device can be used to evaluate the role of specific populations of primary afferents or spinal cord neurons in different sensory modalities, including

pain and itch (Fig. 6). The spinal optoelectronic device can also potentially be used to target specific populations of spinal cord neurons. These studies have the potential to further our understanding of the mechanisms underlying a number of biological processes including proprioception, thermal sensation, mechanosensation, nociception and pruriception.

Evaluation of the analgesic efficacy of novel drugs

The spinal optoelectronic μLED device can be used to efficiently evaluate novel potential analgesic drugs. As shown in Fig. 7, optogenetic stimulation of nociceptive spinal primary afferents with the spinal μLED device can streamline evaluation of analgesic compounds.

Comparison with other methods

Previous approaches using optogenetics to interrogate spinal circuitry have provided critical insights into sensory function but have been limited by the need to tether animals to a light source[15–17]. Tethered approaches present major challenges for the use of optogenetics in a variety of conditions where the attached fibers could interfere with caging, behavioral apparatus and interactions with other animals[18,19]. Optical stimulation approaches that require tethering also have the potential to introduce confounding stress-induced behavioral effects such as stress-induced analgesia[20]. As a result, several approaches have explored wireless options to manipulate spinal cord circuits using optogenetics[3,11,19]. The wireless system described in this protocol allows for evaluation of sensory behaviors induced by optogenetic activation of targeted neuron populations in freely moving mice. This spinal μLED device also provides superior temporal and spatial resolution when compared with chemogenetics or traditional pharmacological approaches[6,14,21]. Light-induced activation of sensory neurons occurs very rapidly using the spinal optogenetic device, as evidenced by the observation of nocifensive behavior within seconds of μLED activation. Other methods, such as chemogenetics and traditional pharmacology, elicit behavior responses that begin over a more protracted time course (several minutes to hours after drug administration). In addition, the combination of genetically restricted expression of an opsin with anatomically targeted μLED illumination provides greater spatial resolution compared with pharmacological and chemogenetic approaches. The greater spatial resolution enabled by our device considerably limits possible off-target effects of neuronal modulation that are unavoidable using these other methods. The use of these devices has the potential to provide critical insights into the complex spinal cord circuitry underlying sensory behavior and pain.

Limitations

The spinal optogenetic device described in this protocol can be used to stimulate neurons or afferents at the thoracic, lumbar and sacral levels of the dorsal spinal cord. This will allow modulation of the activity of spinal dorsal horn neurons or spinal afferents. Stimulation of dorsal horn neurons might be limited by potential confounds related to sufficient light penetration through the parenchyma of the dorsal spinal cord. This can be addressed by the use of higher-intensity μLEDs. We are currently developing tools for this purpose. Due to anatomical constraints, the device is not currently adaptable for implantation at the cervical level of the spinal cord. In addition, the spinal optogenetic device is not adapted for light delivery to the ventral spinal cord.

Lastly, although we have optimized the wireless power harvesting capacity of this device, there are some potential technical limitations. Currently, the maximum area that can be covered by the antenna is a 30 × 30 cm enclosure. Although an arena of this size is adequate for most conventional behavior paradigms, applications requiring a larger arena are currently not feasible. In addition, the consistency of light-mediated stimulation might be impacted by the location and orientation of the animal relative to the antenna wire around the cage. We have shown that the magnetic field distribution in the *XZ* (Supplementary Fig. 2C) and *XY* (Supplementary Fig. 2D) planes remains relatively uniform even at high powers. However, we cannot exclude the possibility that unrestricted movement of the animal within the enclosure could result in momentary positioning of the device in an orientation that does not provide optimal power harvesting. We do not believe that these potential technical limitations will appreciably diminish the utility of the spinal optogenetic device.

Expertise needed to implement the protocol

Implementation of this protocol will be facilitated by prior surgical training. However, we have found that, with practice, the required surgical expertise can be readily attained by motivated investigators. The time required for training is dependent on the ability of the surgeon. The NeuroLux optogenetic

system described in this protocol is user-friendly, and operation of this equipment requires no prior experience. User support and training in the use of the electronic components are available from the manufacturer.

Experimental design

NeuroLux spinal optogenetic device

This protocol details the procedure for use of the NeuroLux spinal optogenetic device for stimulation of spinal afferents. The spinal device and the electronic equipment required for operation of the device are commercially available from NeuroLux (www.neurolux.org). The protocol presented here has two principal components: surgical implantation of the spinal device and activation of the device using the NeuroLux optogenetic system. The specific parameters selected for optimal device activation will depend on a number of factors, including the neuron population that is targeted, the type of light-activated channel that is expressed (e.g., inhibitory or excitatory) and the color of the μLED that is required (e.g., blue or green light, etc.). The stimulation parameters used in this protocol were optimized for activation of nociceptive afferents using the NeuroLux blue spinal device in combination with transgenic expression of the light-sensitive cation channel ChR2. We have used adult male and female mice in these experiments. The device can be implanted in adult mice of any age with a minimum weight of 18 g; the example data we include here were obtained from mice aged 13–21 weeks at the time of device implantation.

Implantation of the NeuroLux spinal optogenetic device

Experimental manipulation of spinal circuits that underlie specific sensory behaviors is achieved by targeting expression of ChR2 or other light-activated proteins (opsins) to appropriate populations of spinal neurons or spinal afferents[13,14]. The utility of this device is contingent on expression of an opsin in spinal dorsal horn neurons or spinal afferents. This can be readily achieved with the use of transgenic mice carrying a conditional allele for the desired opsin, where expression of the conditional allele is dependent on the presence of Cre recombinase in the same cell[22]. Crossing these conditional mice with mice that express Cre recombinase in a targeted population of neurons will generate mice in which the opsin is specifically expressed in the neuron population of interest[3,4,15,16,23]. Alternatively, expression can be achieved by viral transduction of opsin transgenes[12].

The surgical implantation procedure that is detailed below describes implantation of the spinal optogenetic device with the μLED positioned over the lumbar enlargement of the spinal cord in the epidural space for the purpose of stimulating the central processes of nociceptive afferents that innervate the lower limbs and lower trunk (Fig. 2a–e). To target nociceptive afferents, we use mice in which ChR2 is selectively expressed in nociceptive afferents (TRPV1-ChR2 mice). These mice were created by crossing mice with a conditional ChR2 allele (Ai32 mice; Jackson Laboratories, stock no. 012569) with mice that express Cre recombinase from the nociceptor-specific TRPV1 locus (TRPV1-Cre mice; Jackson Laboratories, stock no. 017769)[22,24,25].

Stimulation or inhibition of other populations of spinal afferents or spinal dorsal horn neurons can be achieved by the use of commercially available mouse lines that target Cre recombinase expression to specific neuron populations of interest crossed with mice that harbor a conditional allele for the desired opsin[14,22]. The appropriate control mice will depend upon the specific mouse lines used. Mice that harbor the conditional opsin allele but lack Cre recombinase and therefore do not express the opsin are suitable controls. Littermates of experimental mice are preferred as controls, and these can be obtained from the same crosses that generate experimental mice. Ideally, both experimental mice and control mice should be included in individual experiments where optogenetic stimulation is applied under the same conditions. The effects of optical stimulation should also be evaluated, where possible, in experimental paradigms in which the effect of light stimulation is compared with the effect achieved in the absence of light stimulation in the same animals. This is feasible in behavior studies but may not be possible in anatomical studies. In the examples of proper device function presented below we have used both types of controls.

Materials

Animals

! CAUTION All experiments using mice must comply with institutional guidelines and policies regarding the use of vertebrate animals in research. The surgical and experimental procedures presented

in this manuscript were approved by the Animal Care and Use Committee of Washington University School of Medicine.

- Mice that express a light-activated channel (or other opsin) in specific populations of spinal afferents or spinal dorsal horn neurons. As an example, we use Ai32 (Jackson Laboratories, stock no. 012569) crossed with TRPV1-Cre mice (Jackson Laboratories, stock no. 017769) in this protocol (see Experimental Design). This approach allows us to conditionally express ChR2, an excitatory light-activated cation channel, in neurons that coexpresses Cre recombinase[22]. These mice express Cre recombinase from the nociceptor-specific TRPV1 locus[24,25], allowing for restricted expression of Cre-recombinase mainly in sensory dorsal root ganglia (DRG) neurons that coexpress TRPV1. Homozygous female Ai32 mice were crossed with heterozygous TRPV1-Cre male mice. Experiments were performed on both male and female mice that were Ai32 and TRPV1-Cre positive.
- Littermate control mice lacking the opsin. We used male and female mice that were Ai32 positive but Cre negative in this protocol (see 'Experimental design').

Reagents

- Betadine solution 10% (vol/vol) povidone-iodine (Purdue Products, cat. no. 6761815017)
- Puralube ophthalmic ointment (Patterson Veterinary, cat. no. 07-888-2572)
- Sterile saline (Henry Schein, cat. no. 1048583)
- Super glue gel (Loctite Super Glue Gel Control, item no. 234790)
- Glue accelerator (Hobby Lobby, cat. no. SKU:238766)
- Buprenorphine (Reckitt Benckiser Pharmaceuticals, obtained from WUSM Pharmacy)
- Buprenorphine SR (ZooPharma, obtained from WUSM Pharmacy)

Equipment

- Dissecting microscope (S9i Stereomicroscope; Leica, cat. no. 19450816)
- Deltaphase isothermal pads (Braintree Scientific, cat. no. 39DP)
- Sterile wood applicator sticks (Patterson Veterinary, cat. no. 07-891-7989)
- Sterile cotton-tipped wood applicator sticks (Patterson Veterinary, cat. no. 07-847-3562)
- Gauze sponges (Patterson Veterinary, cat. no. 07-893-8572)
- Glass bead sterilizer (Harvard Apparatus, cat. no. 61-0183)
- Sharpening stone for surgical instruments (Roboz Surgical, cat. no. IN-5)
- Scalpel knife handle #3, 5″ (Biomedical Research Instruments (BRI), cat. no. 26-1000)
- Scalpel blade #10 (BRI, cat. no. 26-1310)
- Small scissor (BRI, cat. no. 11-2030)
- Micro dissecting forceps, 4″ serrated, half curved (BRI, cat. no. 10-2310)
- Dumont pattern #5 forceps (BRI, cat. no. 10-1140) with tips blunted using a sharpening stone
- Micro scissor (BRI, cat. no. 11-1050)
- Micro dissecting forceps, 4″ serrated (BRI, cat. no. 10-2350)
- AUTOCLIP wound clip applier (BRI, cat. no. 43-1000)
- AUTOCLIP 9 mm, box of 100 (BRI, cat. no. 43-1010)
- Custom-made animal enclosure ▲ **CRITICAL** In this protocol, we use a custom-made plexiglass animal enclosure, which is assembled as described in Steps 27 and 28 and requires the following components.
- Plexiglass plates for assembling a 10 × 33 × 10 cm enclosure (custom made by the Washington University School of Medicine machine shop)
- NeuroLux optogenetics system ▲ **CRITICAL** The components below are required for optogenetic stimulation of spinal afferents and are commercially available from NeuroLux (www.neurolux.org).
- Spinal μLED implants (blue μLEDs are used in the examples below; NeuroLux, cat. no. WID-S2A)
- Power distribution control (PDC) box (NeuroLux, cat. no. PDC-2A)
- Autotuner antenna box (NeuroLux, cat. no. TXAMB-1A)
- Laptop with NeuroLux software (NeuroLux, cat. no. PPCC-2A)
- Insulated solid tinned copper wire to wrap around behavioral setup for generation of the near-field communication field (NeuroLux, cat. no. CUW-1A). We used a 22 AWG copper wire in the form of a single parallel double loop placed 3 and 6 cm from the cage floor.

Procedure

▲ **CRITICAL** Figs. 1, 2 and 4 illustrate the principal steps of the procedure. Supplementary Video 1 illustrates Steps 7–22 of the surgical procedure.

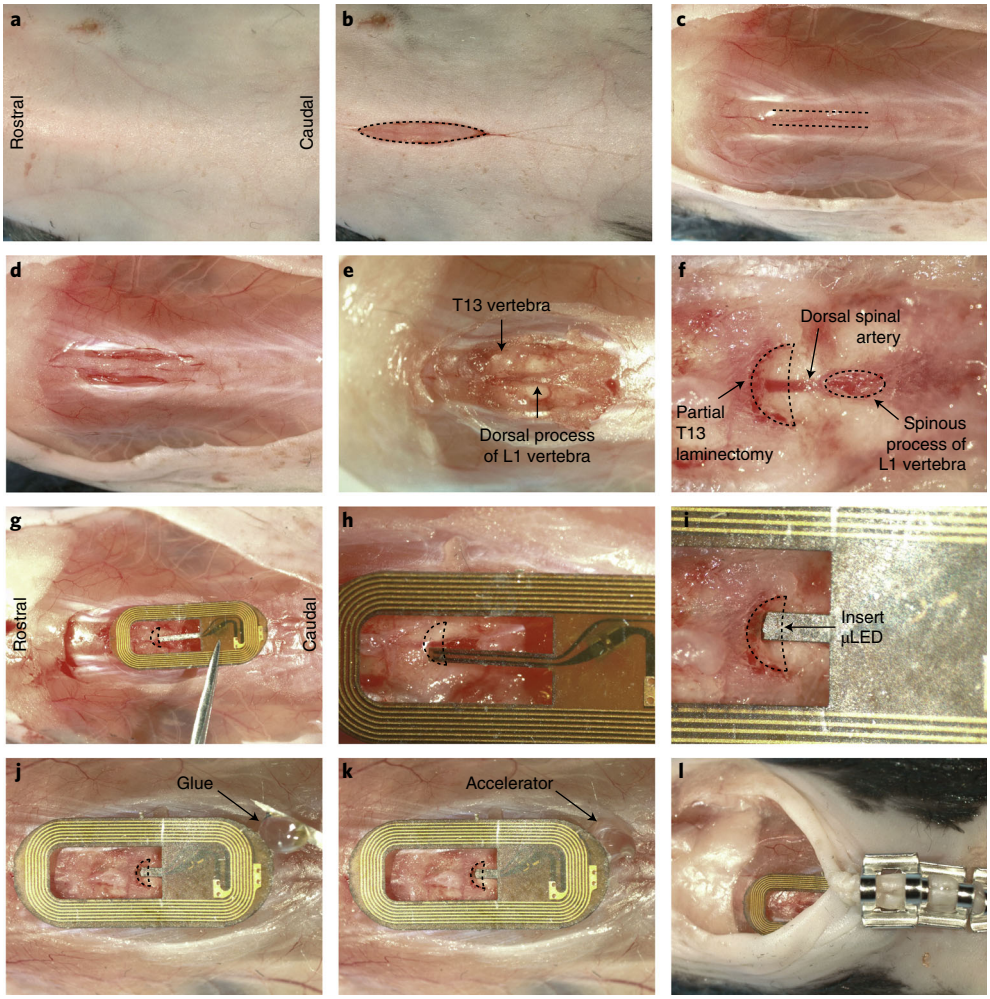

Fig. 4 | Procedure for implantation of the spinal µLED device. a, Clean-shaven area at the site of the skin incision on the back of the mouse (Steps 5 and 6). **b**, Small skin incision made with a #10 scalpel blade (Step 7). **c**, Skin incision extended using small scissor to expose the dorsal back muscles. Black dashed lines indicate the site of muscle incision (Step 8). **d**, Muscle incision just medial to the spinous processes of the vertebral bodies (Steps 9 and 10). **e**, T13 and L1 vertebral bones with overlying muscle removed (Steps 11 and 12). **f**, Partial laminectomy of the T13 vertebral bone outlined with dashed black line. Spinous process of the L1 vertebral bone removed (dashed black line) (Steps 13 and 14). Note the sharp profile of the artery on the dorsal surface of the spinal cord. **g**,**h**, The spinal µLED device with the µLED oriented downward for insertion into the epidural space beneath the T13 vertebral bone (Step 16). **i**, The device probe inserted under the T13 vertebral bone (Step 17). **j**,**k**, The spinal device is adhered to the L1 vertebral body using super glue gel (**j**) and accelerator (**k**) (Steps 18–20). **l**, Closure of the skin incision with closely spaced wound clips (Steps 21 and 22). Experiments shown in this figure comply with the guidelines and policies of the Animal Care and Use Committee of Washington University School of Medicine regarding the use of vertebrate animals in research.

Preoperative preparation ● Timing 10–15 min

1 Sterilize all surgical instruments, gauze sponges, wood applicator sticks and cotton-tipped wood applicator sticks by autoclaving. If surgery is performed on multiple mice within the same session, instruments can be resterilized between mice by first removing all visible material with sterile saline and sterile gauze sponges and then sterilizing instruments with a glass bead sterilizer.

2 Anesthetize the mouse using 2.5% (vol/vol) isoflurane for both induction and maintenance.

3 Place the mouse in a sternal recumbent position on a Deltaphase isothermal pad (under the dissecting microscope).

▲ **CRITICAL STEP** For optimal recovery and survival, it is essential to maintain body temperature during the surgical procedure.

4 Apply Puralube to the eyes to prevent drying of the cornea during surgery.

5 Shave the skin over the vertebral column from the neck to the lower back of the mouse.
▲ **CRITICAL STEP** Take care to shave the mouse cleanly. If hair remains at the site of the skin incision, it will contaminate the surgical field (Fig. 4a).

6 Scrub the skin first with 70% (vol/vol) ethanol followed by betadine solution.

Surgical implantation procedure ● Timing 30–45 min

7 Use a scalpel with a #10 blade to make a small longitudinal incision in the skin over the rib cage at the midline (Fig. 4b).
▲ **CRITICAL STEP** Take care to cut the skin only. Avoid cutting into the underlying muscles.

8 Use a small scissor to extend the skin incision rostrally to the neck and caudally to the pelvic girdle (Fig. 4c).
▲ **CRITICAL STEP** Once the skin is open, keep the cut edges of the skin and the entire surgical field moist throughout the procedure with sterile saline (Fig. 4c).

9 Locate the T13 and L1 vertebrae, which overlie the lumbar enlargement, using the most caudal rib as a landmark. The most caudal rib is attached to the T13 vertebra.

10 Use a second scalpel with a #10 blade to bilaterally cut the superficial muscles of the back (trapezius and latissimus dorsi muscles) at their origin on the spinous processes of the vertebrae and the paraspinous muscles lateral to the spinous processes of the T13 and L2 vertebrae (Fig. 4c,d).
▲ **CRITICAL STEP** Care must be taken to cut the muscles close to the spinous processes of the vertebral bones. Cutting too far lateral to the spinous process might result in cutting through the dorsal abdominal wall.
▲ **CRITICAL STEP** Use a different scalpel from the scalpel used for skin incision. Using the same scalpel for both skin and muscle incision will increase the risk of infection.

11 Use a half-curved micro forceps and a micro scissor to remove the muscle overlying the spinous processes of the vertebrae. Use blunted Dumont #5 forceps to remove all of the soft tissue on the dorsal surface of the T13 and L1 vertebrae. Use sterile saline to irrigate the surgical field and sterile cotton (cotton-tipped applicators and pledgets pulled from cotton-tipped applicators) to remove blood (Fig. 4e).
▲ **CRITICAL STEP** Muscle can be removed with the half-curved micro forceps and/or the blunted Dumont #5 forceps. Do not use forceps to remove fibrous tissue (ligaments). Use micro scissors to cut fibrous tissue. Pulling on fibrous ligaments will exacerbate bleeding.
? TROUBLESHOOTING

12 Carefully remove the soft tissue between the T13 and L1 vertebrae using a blunted Dumont #5 forceps to expose the spinal artery on the dorsal surface of the spinal cord (Fig. 4f).
▲ **CRITICAL STEP** The profile of the dorsal spinal artery on the dorsal surface of the spinal cord should remain sharp throughout the procedure. If the profile becomes fuzzy, the dura or spinal cord might have been damaged. In this case, it is advisable to euthanize the animal.
? TROUBLESHOOTING

13 Use a blunted Dumont #5 forceps to remove the spinous process from the L1 vertebra (Fig. 2a,b). While stabilizing the vertebral column immediately rostral to the L1 vertebra with the thumb and index finger of one hand, use a Dumont #5 forceps held in the other hand to firmly grasp the base of the spinous process of the L1 vertebrae. Use gentle deflection of the forceps to break the spinous process of the L1 vertebra at the base. Use sterile saline and sterile cotton (cotton-tipped applicators and pledgets pulled from cotton-tipped applicators) to remove blood (Fig. 4f).
▲ **CRITICAL STEP** Be sure to remove the detached spinous process from the surgical field.
? TROUBLESHOOTING

14 Use blunted Dumont #5 forceps (filed so that the tips are less fine) to remove small pieces (200 μm) of bone from the caudal edge of the T13 vertebra (Fig. 2a,b). Use sterile saline and sterile cotton (cotton-tipped applicators and pledgets pulled from cotton-tipped applicators) to remove blood (Fig. 4f).
▲ **CRITICAL STEP** Orient the forceps parallel to the spinal cord to avoid damaging the spinal cord with the tips of the forceps.
? TROUBLESHOOTING

15 Use sterile cotton-tipped applicators and sterile saline to clean and dry the dorsal surface of the L1 vertebrae.
▲ **CRITICAL STEP** The dorsal surface of the L1 vertebral bone must be dry and free of debris before glue is applied in Step 18. If the surface of the L1 vertebra is not clean, the device cannot be firmly adhered to the L1 vertebra.
? TROUBLESHOOTING

16 Bend the body of the spinal device slightly and extend the probe as shown in Fig. 1d.

17 Hold the device by using a Dumont #5 forceps to grasp the body of the device (Figs. 1f and 4g). Insert the probe under the T13 vertebra with the μLED facing the dura (Figs. 2d,e and 4h,i). The probe will slide in without resistance. If there is resistance, extend the laminectomy at the caudal edge of the T13 vertebra by removing small pieces of bone as in Step 14 (Fig. 4f).
▲ **CRITICAL STEP** If resistance is encountered when advancing the probe, do not apply force. Application of force might result in damage to the spinal cord.

18 Use a clean, sterile wooden applicator stick to apply super glue gel between the device body and the dorsal surface of the L1 vertebra (Fig. 4j).
? TROUBLESHOOTING

19 Use a clean, sterile wooden applicator stick to apply gentle pressure to the body of the device so that the body of the device is adhered to the L1 vertebra.
? TROUBLESHOOTING

20 Apply accelerator to the edges of the device to set the glue (Fig. 4k).
? TROUBLESHOOTING

21 Irrigate the surgical field thoroughly with sterile saline to remove all visible blood.
▲ **CRITICAL STEP** A clean field will minimize inflammation that might interfere with the function of the device. Before closing the skin, ensure that all visible blood, detached bone and detached muscle is removed from the field. Bleeding may be especially evident at Steps 11–14. When bleeding occurs, it is advisable to pause the surgery until bleeding is controlled. Sterile cotton applied to the site of bleeding followed by irrigation with warm sterile saline will efficiently control bleeding.

22 Hold the cut edges of the skin incision together using a micro dissecting forceps, and close the wound with 9 mm wound clips using an AUTOCLIP wound clip applier with 9 mm AUTOCLIPs (Fig. 4l).
? TROUBLESHOOTING

Postoperative care ● Timing <5 min

23 At the conclusion of surgery, administer 1 ml of warm sterile saline subcutaneously at the nape of the neck.

24 Administer buprenorphine (0.05–0.1 mg/kg) or buprenorphine SR (0.5–1.0 mg/kg) through postoperative day 3.

25 Monitor the mouse continuously until it is recovered from anesthesia and fully ambulatory.
? TROUBLESHOOTING

26 Allow the animals 48–72 h to fully recover from the acute effects of surgery before performing behavior studies.
■ **PAUSE POINT** Once recovery from surgery is complete, optical stimulation can be performed at any time point. We have maintained and stimulated mice with implants for greater than 10 weeks postsurgery.

Optical stimulation ● Timing variable

27 Construct an enclosure suitable for the experiment. In the examples provided below, we used plexiglass enclosures that accommodate two mice (Fig. 6) or a single mouse (Fig. 7).

28 Wire the enclosure using a single parallel double loop of insulated solid tinned copper wire. The wires must be twisted as they exit the enclosure towards the antenna and bifurcate just as they reach the antenna tuner box.

29 Tune the antenna with the autotuner using the instructions provided by the manufacturer. Set the parameters for stimulation using the NeuroLux software. Stimulation parameters include the stimulation frequency (Hz), the pulse duration (ms) and the power output for the antenna. A burst mode feature is available that allows ON/OFF bursting of the μLED.
▲ **CRITICAL STEP** The antenna tuner box maximizes the power transfer between the power distribution control (PDC) box and the enclosure's antenna. Tuning the antenna is necessary to obtain maximal power transfer for the enclosure. The tuning procedure instructions are provided by NeuroLux with the system. Retuning is only required if there are major changes to the antenna's surroundings, such as the presence of another NeuroLux system, contacts with large electronics or if the equipment is moved to a different location. The maximum area that can be covered by the antenna is a 30 × 30 cm enclosure.
? TROUBLESHOOTING

Troubleshooting

Troubleshooting guidance can be found in Table 2.

Table 2 | Troubleshooting Table

Step	Problem	Possible Cause	Solution
11–14	Uncontrolled bleeding	Removing large pieces of bone	Remove smaller amounts of bone in a single forceps bite. When bleeding occurs, pause surgery and apply sterile cotton to the source of blood flow until bleeding is controlled
		Removing fibrous tissue by tearing with forceps	Use forceps to extend fibrous tissue; then use micro scissors to cut fibrous tissue
13, 15, 18–20	Device migration	Device not properly adhered to L1 vertebral bone	Ensure that the dorsal surface of the L1 vertebral bone is clean and dry before applying glue. Apply a sufficient amount of glue and accelerator. Maintain gentle pressure on the body of the device for sufficient time to allow the glue to set
22	Wound dehiscence	Margins of skin incision become desiccated during surgery	Irrigate surgical field frequently with sterile saline to maintain tissue hydration
		Insufficient wound closure	Apply wound clips with less than 3 mm of space between clips
25	Mouse does not recover from anesthesia	Prolonged anesthesia	With practice, the time required to perform the surgical procedure will decrease
		Excessive blood loss during surgery	Control bleeding during surgery. Administer saline immediately after surgery
Post-procedure	Wound infection	Improper sterilization of surgical tools or other materials (i.e., gauze sponges, applicator sticks, saline)	Autoclave tools and materials prior to surgery
		Poor aseptic technique during surgery	Obtain training in proper surgical aseptic technique
	Mouse exhibits altered gait or paralysis after recovery from surgery	Damage to the spinal cord	When performing the laminectomy, orient the forceps parallel to the vertebral column to avoid jabbing the spinal cord with the forceps
	Activation of the device does not elicit the expected behavior	Electronic system is set up incorrectly	Place a test device in the animal enclosure to verify that the system is operational. If the system is not functioning correctly, contact NeuroLux customer support
		Device damaged during surgery	If the device has been damaged, it cannot be repaired. Damage to the device can be avoided by careful handling. We have not observed damage to the device during surgery
		The spinal cord is damaged	When performing the laminectomy, orient the forceps parallel to the vertebral column to avoid jabbing the spinal cord with the forceps

Timing

Steps 1–6, preoperative preparation: 10–15 min
Steps 7–22, surgical implantation procedure: 30–45 min
Steps 23–26, postoperative care: <5 min
Steps 27–29, optical stimulation: variable time

Anticipated results

General effects of spinal optogenetic device implantation on mice

Implantation of the spinal optogenetic device does not affect the general health of mice. We found no significant difference in body weight or in the appearance of implanted male and female mice compared with sham-operated mice ($P > 0.05$; Fig. 5a). In addition, we evaluated the effect of device implantation on sensory behavior. Cold and mechanical sensitivity were evaluated in implanted mice

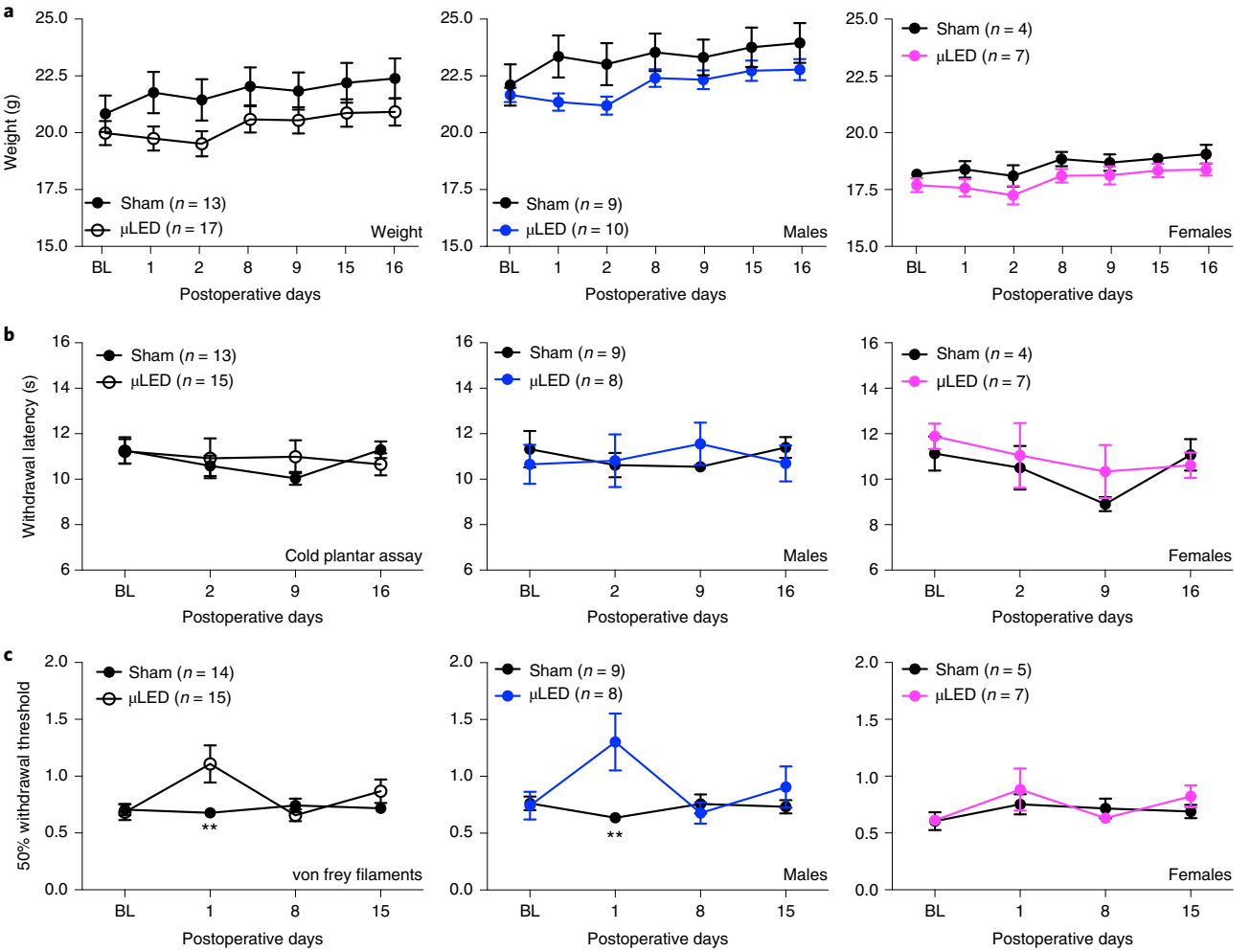

Fig. 5 | General effects of spinal optogenetic device implantation on mice. a, Postimplantation weight (g) after either μLED implantation or sham surgery; all mice (left), male mice only (middle) or female mice only (right). **b**, Postimplantation cold sensitivity (withdrawal latency in seconds) in mice with spinal μLED device implant or sham surgery; all mice (left), male mice only (middle) or female mice only (right). **c**, Postimplantation mechanical sensitivity (withdrawal threshold in g) in mice with spinal μLED device implant or sham surgery; all mice (left), male mice only (middle) or female mice only (right). Analysis of variance performed using a two-way ANOVA for repeated measurements (**$P < 0.001$), data shown as mean ± SEM. The full quantitative data for panels **a**,**b** and **c** are provided in the Source Data associated with this protocol. Power analysis to determine the appropriate size of the behavioral experimental groups was performed to detect differences between two means and was calculated with 99% power, using a two-group *t*-test with a 0.05 two-sided significance level. According to the results of the power analysis, for an effect size of 1.5, we needed 11–12 animals to detect a significant difference. Behavioral experiments were performed in three separate cohorts, as a means to provide replication. Animals were randomized to receive either sham or LED implants. Experimenters were blinded to the experimental conditions during acquisition and analysis when comparisons were made by surgery conditions or genotype. Behavioral experiments were video recorded and manually scored. Experiments shown in this figure comply with the guidelines and policies of the Animal Care and Use Committee of Washington University School of Medicine regarding the use of vertebrate animals in research.

using the cold plantar assay and the von Frey test, respectively[26,27]. Sensitivity to a cold stimulus was not significantly different in male or female mice with spinal device implants compared with sham-operated mice at PID 2, 9 or 16 (Fig. 5b). Mechanical sensitivity was transiently decreased in implanted male mice compared with sham-operated male mice at PID 1 (Fig. 5c). At all other time points evaluated, mechanical sensitivity was not altered in implanted male or female mice compared with sham-operated mice ($P > 0.05$). Post hoc analysis revealed that the decreased mechanical sensitivity observed at PID 1 was present in only two of the eight male mice tested. The limited and transient nature of this deficit suggests that this could be the result of postsurgical inflammation resulting from the laminectomy and not due to the presence of the spinal device.

Light-evoked behavior in mice with spinal optogenetic device implantation

The type of behavior that is elicited by light stimulation using the spinal device is dependent on the population of neurons expressing the opsin and the nature of the opsin that is expressed.

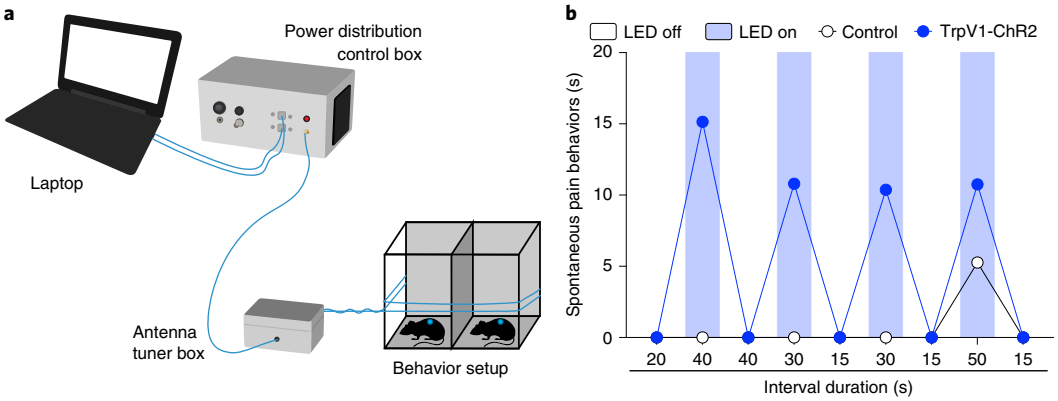

Fig. 6 | Light-evoked pain-like behavior in TRPV1-ChR2 mice. a, Behavioral setup for wireless optogenetic stimulation of nociceptive primary afferents using spinal μLED implants. **b**, Example of light-evoked pain-like behavior in a TRPV1-ChR2 mouse (blue circles) and a control mouse (white circles) upon μLED activation. Intervals during which the μLED is on are depicted by blue bars. Intervals during which the μLED is off are depicted by white bars. The full quantitative data for panels **b** are provided in the Source Data associated with this protocol. Experiments shown in this figure comply with the guidelines and policies of the Animal Care and Use Committee of Washington University School of Medicine regarding the use of vertebrate animals in research.

To determine if the spinal optogenetic device could be used to elicit pain behavior, we targeted expression of ChR2 to nociceptors, the subpopulation of dorsal root ganglion sensory neurons that transmit pain[28]. We crossed mice that have a conditional ChR2 allele that requires Cre recombinase for expression (Ai32 mice) with mice that express Cre recombinase from the TRPV1 locus (TRPV1-Cre mice). TRPV1-ChR2 mice generated from this cross express ChR2 in nociceptors[3,4,28]. Control mice obtained from this cross have the conditional ChR2 allele but lack Cre recombinase, and thus do not express ChR2.

An example experiment that illustrates the equipment setup for optogenetic stimulation (Fig. 6a) and the appropriate performance of the spinal optogenetic device (Fig. 6b) is shown in Fig. 6. We simultaneously recorded light-evoked behavior in a TRPV1-ChR2 mouse and a control mouse at PID 29 (Fig. 6). The spinal optogenetic device was implanted as described above (Procedures), with the blue μLED of the device located in the epidural space at the level of the lumbar enlargement of the spinal cord. Optogenetic stimulation of the TRPV1-ChR2 mouse with blue light at 1 Hz elicited classic pain-like behavior characterized by shaking of the lower limbs and licking and biting of the lower back and limbs[28]. These regions of the body are innervated by sensory afferent neurons with central processes that terminate in the dorsal horn of the spinal cord at the level of the lumbar enlargement where the μLED is located. Pain-like behavior was quantified in these mice during intermittent periods in which the μLED was on or off. The TRPV1-ChR2 mouse exhibited light-induced pain-like behaviors when the μLED was on but not when the μLED was off (Fig. 6b). The control mouse did not exhibit definitive pain-like behavior when the μLED was on or when the μLED was off, demonstrating that activation of the μLED in the absence of ChR2 expression does not elicit pain-like behavior. The above example shows that, as expected, light-induced activation of nociceptors elicits pain-like behavior directed to the body region targeted by μLED placement at the lumbar enlargement. To verify that the observed behavior is a response to pain, we provide an additional example of proper device function that demonstrates that light-induced behavior can be attenuated by the analgesic buprenorphine. Figure 7 illustrates light-induced behavior in a PID 17 TRPV1-ChR2 mouse. In the absence of buprenorphine (Fig. 7a, left panel), light stimulation induces pain-like behavior that is absent when the μLED is not illuminated (as also seen in Fig. 6b). At 30 min after administration of buprenorphine (0.1 mg/kg), pain-like behavior is absent when the μLED is illuminated (Fig. 7b, left panel). The ability of the analgesic buprenorphine to block light-induced behavior indicates that this represents pain-related behavior. At 3 h after buprenorphine administration, pain-related behavior is again observed (Fig. 7c, left panel), but the magnitude is less than that observed in the absence of buprenorphine (Fig. 7a, left panel), suggesting that the analgesic effect of buprenorphine is beginning to wear off at this time point. We repeated this experiment at PID 22 and again observed light-induced pain behavior (Fig. 7a, right panel) that was blocked by buprenorphine (Fig. 7b, right panel). However, in this example, we tested the mouse at 6 h after buprenorphine administration and observed a return of pain behavior (Fig. 7c, right panel) that was of greater

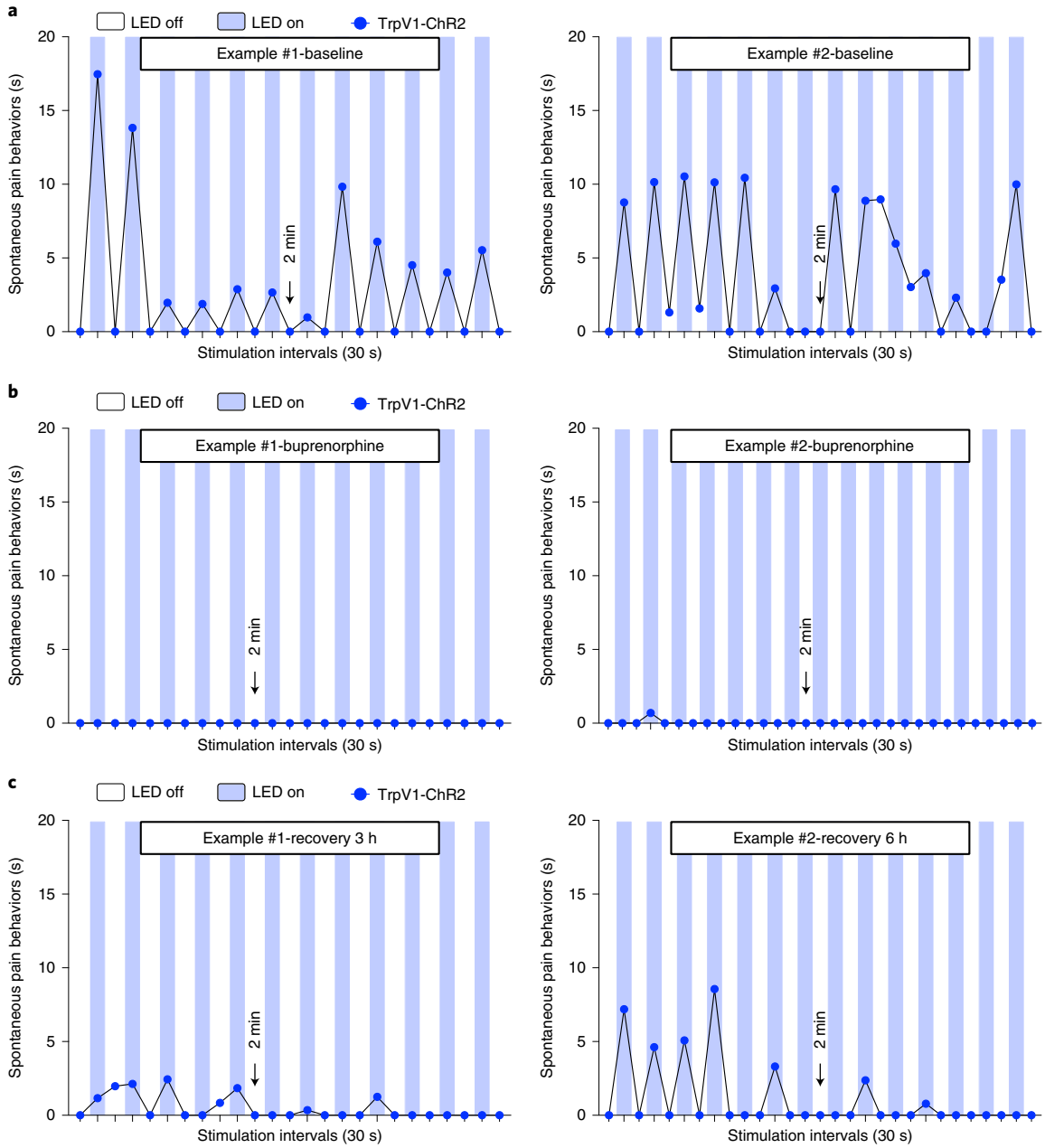

Fig. 7 | Effects of opioid administration on light-evoked pain-like behavior. a–c, Quantification of pain-like behavior in a TRPV1-ChR2 mouse during intermittent periods in which the µLED was on or off observed before buprenorphine administration (**a**), 30 min after buprenorphine administration (**b**), 3 h after buprenorphine administration (left, **c**) or 6 h after buprenorphine administration (right, **c**). Intervals during which the µLED is on are depicted by blue bars. Intervals during which the µLED is off are depicted by white bars. The full quantitative data for panels **a**,**b** and **c** are provided in the Source Data associated with this protocol. Experiments shown in this figure comply with the guidelines and policies of the Animal Care and Use Committee of Washington University School of Medicine regarding the use of vertebrate animals in research.

magnitude than pain behavior observed at 3 h after buprenorphine (Fig. 7c, left panel). The light-induced nocifensive behavior shown in Figs. 6 and 7 are representative examples of device function. When the device is correctly implanted in an animal with ChR2 expression, behavior is consistently elicited upon µLED activation.

Reporting Summary

Further information on research design is available in the Nature Research Reporting Summary linked to this article.

Data availability

Source data are provided with this paper. Additional requests should be addressed to the corresponding authors.

References

1. Boyden, E. S. A history of optogenetics: the development of tools for controlling brain circuits with light. *F1000 Biol. Rep.* **3**, 11 (2011).
2. Carr, F. B. & Zachariou, V. Nociception and pain: lessons from optogenetics. *Front. Behav. Neurosci.* **8**, 69 (2014).
3. Samineni, V. K. et al. Fully implantable, battery-free wireless optoelectronic devices for spinal optogenetics. *Pain* **158**, 2108–2116 (2017).
4. Park, S. I. S. Il et al. Soft, stretchable, fully implantable miniaturized optoelectronic systems for wireless optogenetics. *Nat. Biotechnol.* **33**, 1280–1286 (2015).
5. Zhang, Y. Y. et al. Battery-free, fully implantable optofluidic cuff system for wireless optogenetic and pharmacological neuromodulation of peripheral nerves. *Sci. Adv.* **5**, 1–12 (2019).
6. Vázquez-Guardado, A., Yang, Y., Bandodkar, A. J. & Rogers, J. A. Recent advances in neurotechnologies with broad potential for neuroscience research. *Nat. Neurosci.* **23**, 1522–1536 (2020).
7. Bridges, A. W. & García, A. J. Anti-inflammatory polymeric coatings for implantable biomaterials and devices. *J. Diabetes Sci. Technol.* **2**, 984–994 (2008).
8. Bedi, S. S. et al. Chronic spontaneous activity generated in the somata of primary nociceptors is associated with pain-related behavior after spinal cord injury. *J. Neurosci.* **30**, 14870–14882 (2010).
9. Djouhri, L., Koutsikou, S., Fang, X., McMullan, S. & Lawson, S. N. Spontaneous pain, both neuropathic and inflammatory, is related to frequency of spontaneous firing in intact C-fiber nociceptors. *J. Neurosci.* **26**, 1281–1292 (2006).
10. DeBerry, J. J. et al. Differential regulation of bladder pain and voiding function by sensory afferent populations revealed by selective optogenetic activation. *Front. Integr. Neurosci.* **12**, 1–13 (2018).
11. Montgomery, K. L. et al. Wirelessly powered, fully internal optogenetics for brain, spinal and peripheral circuits in mice. *Nat. Methods* **12**, 969–974 (2015).
12. Iyer, S. M. et al. Virally mediated optogenetic excitation and inhibition of pain in freely moving nontransgenic mice. *Nat. Biotechnol.* **32**, 274–278 (2014).
13. Harding, E. K., Fung, S. W. & Bonin, R. P. Insights into spinal dorsal horn circuit function and dysfunction using optical approaches. *Front. Neural Circuits* **14**, 1–21 (2020).
14. Copits, B. A., Pullen, M. Y. & Gereau, R. W. Spotlight on pain: optogenetic approaches for interrogating somatosensory circuits. *Pain* **157**, 2424–2433 (2016).
15. Francois, A. et al. A brainstem-spinal cord inhibitory circuit for mechanical pain modulation by GABA and enkephalins. *Neuron* **93**, 822–839 (2017).
16. Christensen, A. J. et al. In vivo interrogation of spinal mechanosensory circuits. *Cell Rep* **17**, 1699–1710 (2016).
17. Lu, C. *et al.* Flexible and stretchable nanowire-coated fibers for optoelectronic probing of spinal cord circuits. *Sci. Adv.* https://doi.org/10.1126/sciadv.1600955 (2017).
18. Lu, L. et al. Wireless optoelectronic photometers for monitoring neuronal dynamics in the deep brain. *Proc. Natl Acad. Sci. USA* **115**, E1374–E1383 (2018).
19. Wang, Y. et al. Flexible and fully implantable upconversion device for wireless optogenetic stimulation of the spinal cord in behaving animals. *Nanoscale* **12**, 2406–2414 (2020).
20. Butler, R. K. & Finn, D. P. Stress-induced analgesia. *Prog. Neurobiol.* **88**, 184–202 (2009).
21. Mickle, A. D. & Gereau, R. W. 4th A bright future? Optogenetics in the periphery for pain research and therapy. *Pain* **159**, 65–73 (2018).
22. Madisen, L. et al. A toolbox of Cre-dependent optogenetic transgenic mice for light-induced activation and silencing. *Nat. Neurosci.* **15**, 793–802 (2012).
23. Bonin, R. P. et al. Epidural optogenetics for controlled analgesia. *Mol. Pain* **12**, 1–11 (2016).
24. Mishra, S. K., Tisel, S. M., Orestes, P., Bhangoo, S. K. & Hoon, M. A. TRPV1-lineage neurons are required for thermal sensation. *EMBO J* **30**, 582–593 (2011).
25. Cavanaugh, D. J. et al. Restriction of transient receptor potential vanilloid-1 to the peptidergic subset of primary afferent neurons follows its developmental downregulation in nonpeptidergic neurons. *J. Neurosci.* **31**, 10119–10127 (2011).
26. Chaplan, S. R., Bach, F. W., Pogrel, J. W., Chung, J. M. & Yaksh, T. L. Quantitative assessment of tactile allodynia in the rat paw. *J. Neurosci. Methods* **53**, 55–63 (1994).
27. Brenner, D. S., Golden, J. P. & Gereau, R. W. IV A novel behavioral assay for measuring cold sensation in mice. *PLoS ONE* https://doi.org/10.1371/journal.pone.0039765 (2012).
28. Beaudry, H., Daou, I., Ase, A. R., Ribeiro-Da-Silva, A. & Séguela, P. Distinct behavioral responses evoked by selective optogenetic stimulation of the major TRPV1+ and MrgD+ subsets of C-fibers. *Pain* **158**, 2329–2339 (2017).
29. Rogers, J. A. et al. Injectable and injectable cellular-scale electronic devices. US patent 5861366 (2020).

Acknowledgements

We thank J. Sinn-Hanlon for generating the illustrations in Fig. 2. This work was supported by NIH grants NS042595 to R.G., NS103472-02 to J.G.R., DA049569 to B.C. and NEUROLUX SBIR GRANT 5R44MH114944-02.

Author contributions

J.P.G. and R.W.G. developed the surgical approach. B.A.C. performed electrophysiology experiments. J.G.G. performed sensory behavior experiments. J.G.G. and J.P.G. performed optogenetic experiments. S.K.V. maintained and genotyped mice used in these studies. R.A. and Y.H. provided support with computer modeling for μLED device functioning. J.A.R, A.R.B., F.L. and Y.Y. designed and implemented all of the updates to the spinal μLED device in addition to providing technical support. All authors contributed to writing and editing the manuscript.

Competing interests

A.R.B., R.W.G. and J.A.R. are cofounders of NeuroLux. F.L. and Y.Y. work for NeuroLux, a company that manufactures wireless optoelectronic devices. The device described here is included in the current NeuroLux portfolio[29].

Additional information

Supplementary information The online version contains supplementary material available at https://doi.org/10.1038/s41596-021-00532-2.

Correspondence and requests for materials should be addressed to R.W.G.IV. or J.P.G.

Peer review information *Nature Protocols* thanks Maysam Ghovanloo, Ryan Koppes and the other, anonymous reviewer(s) for their contribution to the peer review of this work.

Reprints and permissions information is available at www.nature.com/reprints.

Publisher's note Springer Nature remains neutral with regard to jurisdictional claims in published maps and institutional affiliations.

Received: 6 August 2020; Accepted: 4 March 2021;
Published online: 24 May 2021

Related links

Key references using this protocol

Samineni, V. K. et al. *Pain* **158**, 2108–2116 (2017): https://doi.org/10.1097/j.pain.0000000000000968
Park, S. I. et al. *Nat. Biotechnol.* **33**, 1280–1286 (2015): https://doi.org/10.1038/nbt.3415
Vázquez-Guardado, A. et al. *Nat. Neurosci.* **23**, 1522–1536 (2020): https://doi.org/10.1038/s41593-020-00739-8
Zhang, Y. et al *Sci. Adv.* **5**, eaaw5296 (2019): https://doi.org/10.1126/sciadv.aaw5296

nature research

Corresponding author(s): Judy P. Golden & Robert W. Gereau

Last updated by author(s): Nov 28, 2020

Reporting Summary

Nature Research wishes to improve the reproducibility of the work that we publish. This form provides structure for consistency and transparency in reporting. For further information on Nature Research policies, see our Editorial Policies and the Editorial Policy Checklist.

Statistics

For all statistical analyses, confirm that the following items are present in the figure legend, table legend, main text, or Methods section.

n/a	Confirmed	
☐	☒	The exact sample size (*n*) for each experimental group/condition, given as a discrete number and unit of measurement
☐	☒	A statement on whether measurements were taken from distinct samples or whether the same sample was measured repeatedly
☐	☒	The statistical test(s) used AND whether they are one- or two-sided *Only common tests should be described solely by name; describe more complex techniques in the Methods section.*
☐	☒	A description of all covariates tested
☐	☒	A description of any assumptions or corrections, such as tests of normality and adjustment for multiple comparisons
☐	☒	A full description of the statistical parameters including central tendency (e.g. means) or other basic estimates (e.g. regression coefficient) AND variation (e.g. standard deviation) or associated estimates of uncertainty (e.g. confidence intervals)
☒	☐	For null hypothesis testing, the test statistic (e.g. *F*, *t*, *r*) with confidence intervals, effect sizes, degrees of freedom and *P* value noted *Give P values as exact values whenever suitable.*
☒	☐	For Bayesian analysis, information on the choice of priors and Markov chain Monte Carlo settings
☒	☐	For hierarchical and complex designs, identification of the appropriate level for tests and full reporting of outcomes
☒	☐	Estimates of effect sizes (e.g. Cohen's *d*, Pearson's *r*), indicating how they were calculated

Our web collection on statistics for biologists contains articles on many of the points above.

Software and code

Policy information about availability of computer code

Data collection	Behavioral experiments were video recorded, and manually scored. Data was organized in Microsoft Excel for further analysis. Electrophysiological recordings were made using Patchmaster software controlling a HEKA EPC10 amplifier.
Data analysis	All data was analyzed using PRISM 8.0V. Supplemental video was edited using iMovie version 10.2.1.

For manuscripts utilizing custom algorithms or software that are central to the research but not yet described in published literature, software must be made available to editors and reviewers. We strongly encourage code deposition in a community repository (e.g. GitHub). See the Nature Research guidelines for submitting code & software for further information.

Data

Policy information about availability of data

All manuscripts must include a data availability statement. This statement should provide the following information, where applicable:

- Accession codes, unique identifiers, or web links for publicly available datasets
- A list of figures that have associated raw data
- A description of any restrictions on data availability

The raw data generated during the current study are available as source data files in the form of excel files packaged with this manuscript. Additional requests should be addressed to the corresponding authors.

Field-specific reporting

Please select the one below that is the best fit for your research. If you are not sure, read the appropriate sections before making your selection.

☒ Life sciences ☐ Behavioural & social sciences ☐ Ecological, evolutionary & environmental sciences

For a reference copy of the document with all sections, see nature.com/documents/nr-reporting-summary-flat.pdf

Life sciences study design

All studies must disclose on these points even when the disclosure is negative.

Sample size	Power analysis to determine the appropriate size of the behavioral (Figure 5) experimental groups was performed to determine differences between two means and was calculated with a 99% power, using a two group t-test with a 0.05 two-sided significance level. According to the results of the power analysis, for an effect size of 1.5, we need 11-12 animals to detect a significant difference.
Data exclusions	No data was excluded from this article.
Replication	Behavioral experiments (Figure 5) were performed in 3 separate cohorts, as means to provide replication.
Randomization	Animals were randomized to receive either sham or LED implants (Figure 5).
Blinding	Experimenters were blinded to the experimental conditions, during acquisition and analysis when comparisons were made by surgery conditions or genotype.

Reporting for specific materials, systems and methods

We require information from authors about some types of materials, experimental systems and methods used in many studies. Here, indicate whether each material, system or method listed is relevant to your study. If you are not sure if a list item applies to your research, read the appropriate section before selecting a response.

Materials & experimental systems

n/a	Involved in the study
☒	☐ Antibodies
☒	☐ Eukaryotic cell lines
☒	☐ Palaeontology and archaeology
☐	☒ Animals and other organisms
☒	☐ Human research participants
☒	☐ Clinical data
☒	☐ Dual use research of concern

Methods

n/a	Involved in the study
☒	☐ ChIP-seq
☒	☐ Flow cytometry
☒	☐ MRI-based neuroimaging

Animals and other organisms

Policy information about studies involving animals; ARRIVE guidelines recommended for reporting animal research

Laboratory animals	We used both male and female animals (mus musculus), 8-10 weeks old. Mice were generated by crossing a mouse that expressed conditional ChR2 allele (Ai32 mice; Jackson Laboratories, Stock No: 012569) with mice that express Cre recombinase from the nociceptor-specific TRPV1 locus (TRPV1-Cre mice;, Stock No: 017769). Experimental animals were both positive for the conditional allele and Cre recombinase (TrpV1-ChR2), and control mice only expressed the conditional allele but did not express Cre recombinase.
Wild animals	This study did not involve wild animals.
Field-collected samples	This study did not involve field-collected samples.
Ethics oversight	The surgical and experimental procedures presented in this manuscript were approved by the Animal Care and Use Committee of Washington University School of Medicine.

Note that full information on the approval of the study protocol must also be provided in the manuscript.